Dynamics of the Gulf Stream/Deep Western Boundary Current Crossover. Part I: Entrainment and Recirculation*

MICHAEL A. SPALL

Woods Hole Oceanographic Institution, Woods Hole, Massachusetts

(Manuscript received 27 January 1995, in final form 22 August 1995)

ABSTRACT

A regional primitive equation model is applied to the study of the interaction between the Gulf Stream and the deep western boundary current (DWBC) where they cross at Cape Hatteras. It is found that for a wide range of forcing parameters the upper core of the DWBC is split into two mean paths at the crossover, one flowing toward the south along the western boundary and the other flowing toward the east under the Gulf Stream. The eastward branch is entrained into the southern recirculation gyre and, after being diverted into the interior for up to 1500 km, eventually returns to the western boundary current and continues to flow southward. This recirculation and mixing is shown to have a significant impact on the separation point and mean path of the Gulf Stream, the basin-scale stratification, and the properties of the DWBC south of the crossover. For most configurations, the lower DWBC remains largely on the western boundary and interacts only weakly with the interior. The entrainment of the upper core is shown to be driven by a baroclinic, time-dependent process of DWBC water eddy formations into the recirculation gyres under the Gulf Stream. Potential vorticity considerations are key to understanding the entrainment mechanism and its sensitivity to variations in the model forcing and configuration. A scaling estimate of the amount of entrained DWBC water as a function of the eddy field is derived. The mean paths of the upper and lower DWBCs and strength of the eddy fluxes compare well with various observational estimates. The importance of such entrainment and mixing processes on large-scale ocean modeling and climate studies is discussed.

1. Introduction

The crossover region between the Gulf Stream and the deep western boundary current (DWBC) near Cape Hatteras in the North Atlantic Ocean is unique in that it provides a narrowly confined region through which much of the thermohaline circulation passes. The upper ocean Gulf Stream leaves the shelf carrying warm, salty water northeastward toward high latitudes. The DWBC system transports several water masses of high latitude, convective origin toward low latitudes (Watts 1991; Pickart 1992). It is this northward transport of warm water and compensating southward transport of cold waters that gives rise to much of the net northward heat transport in the North Atlantic. A dynamical understanding of how these intermediate and deep waters move through the system and mix with other water masses is necessary in order to model, monitor, and understand the role of the oceans in the global climate system.

The properties of the DWBC are of considerable interest for the monitoring and understanding of the oceans role in climate (Fine 1995). It is expected that changes in the atmospheric forcing will influence the rate and properties of waters formed at high latitudes and that signals of such changes in the atmosphere might be seen downstream in the DWBC. Thus, monitoring the properties of the DWBC may provide an efficient means to monitor fluctuations in the strength of the thermohaline circulation. In order to relate these fluctuations to changes at the source region, a dynamical basis for how the waters of the DWBC travel down the western boundaries and interact with the ocean interior is required. Recent estimates of the age of the DWBC water based on tracer measurements indicates an effective advection speed in the DWBC of 1–2 cm s^{-1} (Fine 1995; Doney and Jenkins 1994; Pickart et al. 1989). However, direct measurements of the advection speeds in the DWBC give speeds on the order of 5–20 cm s^{-1} (Pickart and Smethie 1993; Watts 1991; Fine and Molinari 1988). This difference between the direct and indirect estimates has been attributed to mixing and exchange processes along the path of the DWBC; however, the locations, forcing mechanisms, and consequences of such exchanges are not well understood. It will be shown here that the Gulf Stream/DWBC crossover is a region of intense mixing that alters the properties of both the Gulf Stream and

* Woods Hole Oceanographic Institution Contribution Number 9013.

Corresponding author address: Dr. Michael A. Spall, Dept. of Physical Oceanography, Woods Hole Oceanographic Institution, Clark 311A, Woods Hole, MA 02543.

the DWBC on the basin scale and, at least for the upper DWBC, can account for the discrepancy between the direct and indirect estimates of the DWBC advection speed.

Several previous analytical and numerical modeling studies of the crossover have treated it as a two-layer system with the Gulf Stream confined to the upper layer and the DWBC confined to the deeper layer. Hogg and Stommel (1985) used a simple steady analytic model to demonstrate how the DWBC could flow under the Gulf Stream at the crossover point while conserving its potential vorticity by sliding down the topographic slope. Thompson and Schmitz (1989, hereafter TS89) studied the influences of the DWBC on the Gulf Stream path in a regional two-layer primitive equation model. They found that the presence of a DWBC shifted the separation point of the Gulf Stream southward and moved the region of maximum eddy activity eastward. Agra and Nof (1993) solved one- and two-layer systems analytically to investigate the influence of opposing baroclinic currents on the separation characteristics. They found that steady solutions were possible only for very special cases and that even very weak opposing boundary currents could strongly affect the separation angle of the stronger boundary current. Cessi (1991) demonstrated the importance of diffusive processes in the separation of opposing barotropic currents in a steady quasigeostrophic system. Ezer and Mellor (1992) found that the presence of a barotropic northern recirculation gyre caused the Gulf Stream to separate farther south, in better agreement with observations, in a regional baroclinic primitive equation model.

Observations indicate that the interaction between the Gulf Stream and the DWBC system is more complicated than can be represented in simple one- or two-layer systems. Pickart (1992), Watts (1991), and Pickart and Smethie (1993, hereafter PS93) have shown that the DWBC is not composed of a current confined to a single layer, nor is it a barotropic recirculation gyre, but rather it is composed of several different water masses that extend up to 700-m depth in the water column. In addition to water masses of convective origin, there is a strong barotropic component that is probably partially wind driven. Pickart and Smethie find that the uppermost portion of the DWBC strongly interacts with the Gulf Stream transport coming off the shelf and appears to be entirely turned offshore at the crossover (at approximately 800-m depth). Slightly deeper (1200 m), the flow appears to be split into two branches, one continuing to the south along the western boundary and the other flowing to the east under the Gulf Stream. The deepest component of the DWBC (3000 m) is estimated to remain over the sloping topography and cross under the Gulf Stream toward the south. It will be shown here that all of the essential characteristics observed by PS93 are represented in the present three-layer model.

The present study has been motivated by these recent observations and by the important role of the thermohaline circulation in the global climate system. Specific questions to be addressed include the following: How are the Gulf Stream and DWBC influenced by the crossover point at Cape Hatteras? What processes control the pathways of the DWBC and its possible entrainment into interior recirculation gyres? What are the consequences of these processes on the properties of both the Gulf Stream and the DWBC? Can mixing and entrainment at the crossover account for the differences in direct and indirect velocity estimates for the DWBC? What process is responsible for the observed splitting of the upper DWBC and lack of splitting in the lower DWBC? These issues are addressed using a regional primitive equation model. The general philosophy for the model design is to conduct the study in parameter space relevant to the real North Atlantic Ocean, yet make simplifying assumptions whenever possible in order to eliminate all but the fundamental elements of the problem. The basic model configuration and forcing is introduced in section 2. The model results, parameter sensitivities, and discussion of the controlling physics is presented in section 3. The relationship of these results to various observations are discussed in section 4 and conclusions are given in section 5.

2. Model configuration and forcing

The model used in this study is based on the regional Gulf Stream model described by TS89. The model solves the primitive equations of motion using an isopycnal vertical coordinate (model equations are given in the appendix). Primitive equations are appropriate for the present study because both the variations in bottom topography near the DWBC and the isopycnal displacements near the Gulf Stream are large compared to the layer thicknesses. The isopycnal formulation also offers a conceptual advantage for process-oriented analysis in that the diapycnal mixing can be set to zero. This allows for near conservation of potential vorticity following fluid parcels and lends itself well to the study of flow pathways within distinct water-mass layers using potential vorticity budgets. In addition to the conceptual advantages of the adiabatic limit, scaling arguments suggest that the influences of diapycnal mixing are likely to be small (see section 3b), and there is little observational or theoretical guidance from which to specify the strength of mixing.

Away from the inflow/outflow regions, the lateral boundaries are vertical walls with boundary conditions of no normal flow and no slip. The transport is specified at inflow points, while at outflow points the normal component of the transport is determined by a radiation condition on the transport in each layer, as described by TS89 and summarized in the appendix. Because the model is adiabatic, the total transport specified to flow into each layer must flow out the open boundary

regions within that layer. There is no mass exchange between layers or temporal storage within the layers.

The model domain is a rectangle 2500 km in latitudinal extent and 3500 km in longitudinal extent with a uniformly slanted coastline along the northwestern portion of the domain, representing the coast of North America, as shown in Fig. 1. (Calculations with a straight western boundary indicate that the basic characteristics of the crossover behavior are not sensitive to this slanted coastline.) The horizontal grid resolution is 25 km in both zonal and meridional directions. The Coriolis parameter varies linearly with latitude as $f = f_0 + \beta y$ with $\beta = 2 \times 10^{-11}$ m^{-1} s^{-1}. The Coriolis parameter at the southern extent of the model domain is $f_0 = 0.616 \times 10^{-4}$ s^{-1}, consistent with a latitude of 25°N. For most calculations, the maximum bottom depth is 5000 m and flat over the entire interior except for a continental slope 250 km wide along the western boundary between 2500-m and 5000-m depth (uniform slope of 0.01 m/m). The Laplacian viscosity is 150 m^2 s^{-1} and the bottom drag coefficient is 0.005 for all experiments.

The surface wind stress is applied in the zonal direction only and given by the analytic function

$$\tau_x = \begin{cases} -\tau_m \cos(y\pi/L), & y < y_m \quad (1) \\ \tau_m\{1 + \cos[(y - y_m)\pi/(L - y_m)]\}/2, & \\ \qquad\qquad y > y_m. \quad (2) \end{cases}$$

The zero wind stress curl occurs at a latitude $y_m = 1200$ km, while τ_m is the maximum value of the zonal wind stress. This wind stress approximately represents the zonal average of the zonal component of the annual mean wind stress over the North Atlantic, the meridional distribution is indicated in Fig. 1 for $\tau_m = 1.0$ dyn cm^{-2}.

The model is also forced through inflow/outflow boundary conditions at the edges of the model domain. An inflow in the upper layer along the western boundary centered at 925-km latitude of width 125 km represents that component of the Gulf Stream transport that leaves the shelf at Cape Hatteras. An inflow angle of 45° (parallel to the bottom topography) is used for all calculations. In the real ocean, this transport is composed of both the wind-driven Sverdrup transport in the North Atlantic and also a component of Southern Hemisphere origin that represents part of the thermohaline circulation (Schmitz and McCartney 1993). No attempt is made to distinguish between these separate sources in the present study. The outflow boundary conditions in layer 1 require that the same amount of transport that enters through the western boundary must leave the domain somewhere through the eastern boundary (the entire eastern boundary is open). There is also a 250-km wide inflow specified in layers 2 and 3 along the northern boundary centered at 1725 km longitude over the sloping bottom. These inflows represent the upper and lower components of the DWBC that are formed at high latitudes. The present model is adiabatic, so the thermodynamics that are responsible for converting the warm Gulf Stream waters into the cold DWBC waters are not explicitly represented in this model, but rather left to be specified through the boundary conditions. The DWBC waters are required to exit the model domain through the southern boundary such that total mass within each layer is conserved. For brevity, the value of the inflow boundary conditions will be specified as $\Gamma = (\Gamma_1, \Gamma_2, \Gamma_3)$, where Γ_k is the transport specified in layer k.

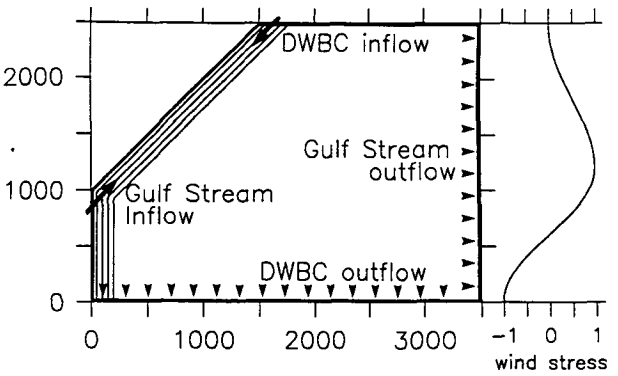

FIG. 1. Model domain and forcing configuration.

In addition to the dynamically active variables of momentum and layer thickness, an age tracer has also been integrated in the model. This tracer is advected within each layer by the horizontal velocity field and also has a parameterization of subgrid-scale mixing processes represented by a Laplacian diffusion operating on the tracer variable (e.g., see Thiele and Sarmiento 1990 for a discussion of age tracers). The diffusion coefficient used for each of the calculations is 50 m^2 s^{-1}. The tracer is initialized with a value of zero everywhere in the model domain and is maintained at a value of zero at the DWBC inflow in layers 2 and 3. In addition to being advected and diffused, the tracer also accumulates time at the rate of 1 unit per year. The value of the age tracer is representative of the age of water parcels since they entered the basin from high latitudes in the DWBC. Of course, the mean age tracer will reflect changes in age due to time-dependent mixing processes, so it is not correct to interpret the age tracer as an exact measure of time since a particular parcel was introduced into the basin.

The model is initialized at rest and integrated for a period of 20 years. The potential density of each of the layers is 26.25, 27.75, and 27.88. These layers represent the main thermocline, the upper component of the DWBC and the lower component of the DWBC. The actual DWBC is composed of more water masses than can be represented in a three-layer model (Pickart

1992). The present vertical resolution has been chosen as the most simple extension of the two-layer model that demonstrates the important consequences of decoupling the middle water masses from the bottom topography. However, one could think of the upper DWBC as the Labrador Sea Water and of the lower DWBC as the lower North Atlantic Deep Water. The resting layer thicknesses are 850 m, 900 m, and 3250 m. This stratification has been chosen to be representative of the observed stratification in the North Atlantic, within the constraints of a three-layer model and the requirement that the layer thicknesses not vanish during the course of integration. The first internal deformation radius at the central latitude of the model domain is 41 km.

There are several points that need to be made with regards to the constraint that the model layer thicknesses not vanish. The wind stress is applied as a body force over the depth of the upper layer, rather than over a much shallower vertical scale associated with an upper mixed layer. The vertical distribution of the wind stress has been shown to influence the separation point in some idealized numerical experiments by Chassignet and Gent (1991). The ability of the upper layer to outcrop has also been shown by Chassignet and Bleck (1993) to influence the separation point in double gyre wind-driven experiments. The continental slope along the western boundary is directly felt only by the deepest layer in the present configuration; however, in the real ocean all layers directly impinge on the bottom where they intersect the western boundary. While it is recognized that each of these physical processes may be important in the full simulation of the Gulf Stream system, they are neglected here in order to obtain a system that is computationally and conceptually manageable. Furthermore, the present study is not intended to be predictive of the real ocean as much as it is to better understand issues related to the middepth interaction between the upper DWBC and the main thermocline. The results of this study provide insight into dynamical processes that may then be applied to the study, and possible improvement, of more complex and comprehensive ocean models.

3. Model results and analysis

There is a great deal of parameter space to explore in such a complicated model and a comprehensive discussion of such an exploration is not attempted here. Rather, the basic sensitivities of the circulation patterns and exchange between the DWBC and interior to variations in the forcing parameters will be presented. Calculations at 50% larger grid spacing give qualitatively the same results so it is believed that the essential aspects of the problem are represented at the present resolution; however, quantitative details of the solutions would probably change at higher horizontal resolution.

a. The central case: Γ = (25, 10, 10), τ_m = 0.75

1) TRANSPORT STREAMFUNCTION

Results from a single calculation with parameters typical of those found in the real North Atlantic will first be presented. The maximum wind stress applied was $\tau_m = 0.75$ dyn cm^{-2}. The inflow transport of the Gulf Stream was specified to be 25 Sv (Sv $\equiv 10^6$ m^3 s^{-1}), while the DWBC transports in layers 2 and 3 are both 10 Sv. The depth integrated mean transport streamfunction is shown in Fig. 2a. The Gulf Stream is represented by a narrow zonal flow along 900-km latitude flanked to the north and south by recirculation

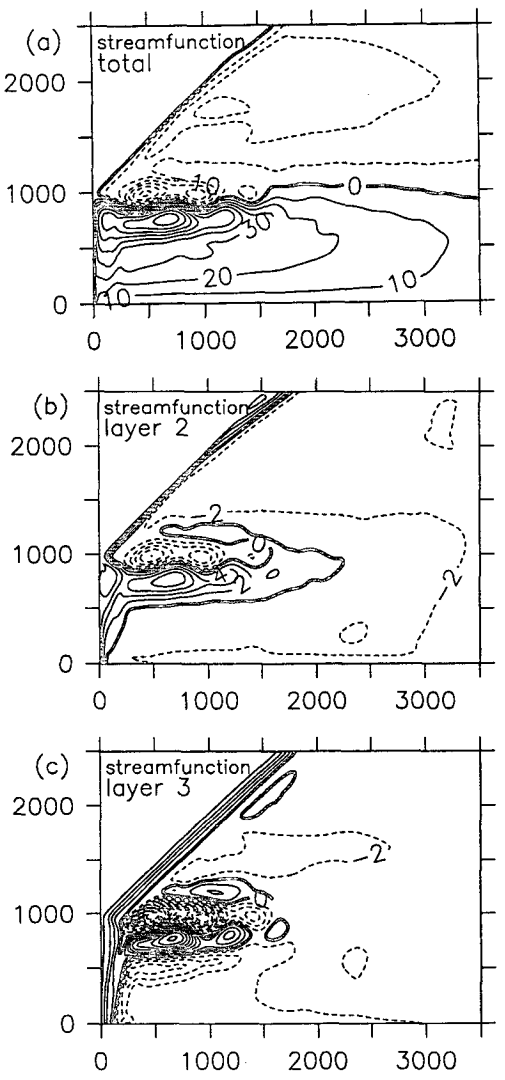

FIG. 2. Time averaged fields (years 15 to 20) for the central case with τ_m = 0.75, Γ = (25, 10, 10): (a) depth-integrated transport streamfunction (Sv $\equiv 1 \times 10^6$ m^3 s^{-1}), (b) transport streamfunction for layer 2, and (c) transport streamfunction for layer 3. Dashed lines indicate negative values.

gyres extending approximately 1500 km into the basin. The latitude of Gulf Stream separation is south of the zero wind stress curl line (1200 km) in part due to the presence of the upper DWBC, as is discussed further in section 3c. The recirculation gyres are driven by the downward flux of momentum as a result of eddy fluxes along the Gulf Stream, as demonstrated by Holland (1978) and Holland and Rhines (1980), and discussed further in Part II of this study (Spall 1996). The Gulf Stream becomes somewhat diffuse east of the recirculation gyres. The maximum zonal transport is approximately 140 Sv with the northern and southern recirculation gyres carrying approximately 30–60 Sv each. Also evident is the transport of the DWBC entering from the northern boundary near 1700-km longitude and exiting the domain along the southern boundary, primarily through the southwest corner. A strong wind-driven anticyclonic circulation is found in the subtropical gyre, while a weaker cyclonic circulation is present in the subpolar gyre. This general circulation pattern is not sensitive to the domain size, provided that it is larger than the extent of the northern and southern recirculation gyres, so it is believed that finite domain size is not strongly controlling the solution in the model interior.

The mean transport streamfunction for layer 2 only is shown in Fig. 2b. The intermediate depth circulation is dominated by the DWBC entering through the northern boundary and the recirculation gyres north and south of the Gulf Stream. There is no direct inflow of Gulf Stream water at this depth, as is consistent with the vertical structure of the observed Gulf Stream (PS93). Each of the recirculation gyres carries about 10 Sv in this layer. The mean transport of the upper core of the DWBC is split into three paths: Approximately 3 Sv flows to the south along the western boundary, although it does shift off the boundary by about 200 km at the crossover. Approximately 5 Sv of DWBC water is entrained into the southern recirculation gyre at the crossover point and returns to the western boundary south of the recirculation gyre. A final 1–2 Sv leaves the western boundary north of the crossover and flows into the basin interior. This transport is required to flow out the southern boundary because the eastern boundary is closed for this layer. However, the flow pattern suggests that, if permitted, this transport would continue to flow to the east under the Gulf Stream. This splitting of the upper DWBC at the crossover is remarkably similar to the estimated flow trajectories based on synoptic data by PS93, as discussed further in section 4.

The mean transport streamfunction for the deepest layer is shown in Fig. 2c. Again, the flow is dominated by the DWBC and recirculation gyres. There is much less interaction between the DWBC and the interior in the deep layer as most of the DWBC transport continues to flow southward over the topography, remaining adjacent to the interior recirculation gyres. The northern and southern recirculation gyres carry approximately 30 Sv and 15 Sv, respectively. The weak interaction of the deep DWBC with offshore recirculation gyres is again consistent with the estimates of PS93 based on synoptic data.

2) Potential vorticity

The mean potential vorticity $Q = (f + \bar{\zeta})/H$ for layer 2 is shown in Fig. 3a, where $\bar{\zeta} = V_x - U_y$ is the mean relative vorticity, U and V are the mean horizontal velocities, and H is the mean layer thickness. The upper core of the DWBC is indicated by the narrow band of low Q along the western boundary. There is also a band of high potential vorticity just off shore of the DWBC. A small tongue of low potential vorticity leaves the boundary at the crossover and flows approximately 200 km toward the basin interior before returning to the western boundary and exiting the domain through the southwest corner. This general pattern indicates a primarily advective regime along much of the DWBC. However, it is evident that the branch of the DWBC that turns to the east and flows under the Gulf Stream crosses the mean potential vorticity contours, suggesting that some diffusive process is active there. The region under the Gulf Stream has nearly homogeneous Q, as predicted by the theory of Rhines and Young (1982) and found in the modeling study of Holland et

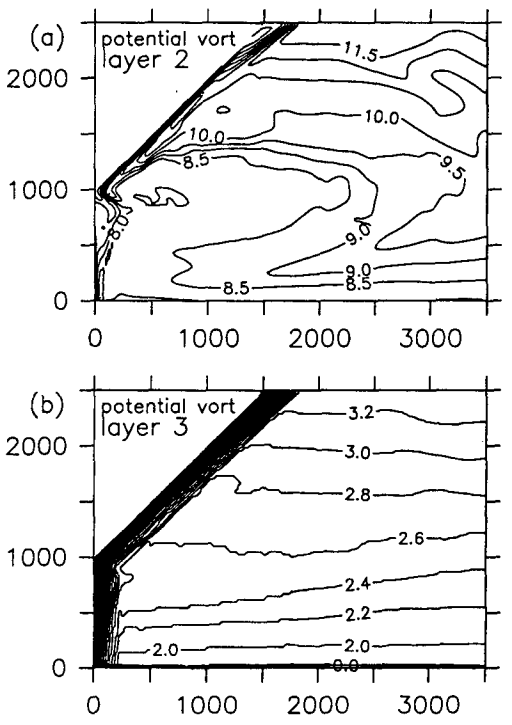

FIG. 3. Time averaged potential vorticity fields (years 15 to 20) for the central case with $\tau_m = 0.75$, $\Gamma = (25, 10, 10)$: (a) layer 2 and (b) layer 3 (units 10^{-8} m^{-1} s^{-1}).

al. (1984) and in historical data by McDowell et al. (1982). Johns (1988) found that the meridional gradient of the potential vorticity is nearly zero (slightly positive local maximum) at a depth of 1000 m in the isopycnal layer of the upper DWBC water. It appears, and will be demonstrated later, that the low Q water under the Gulf Stream in the model is supplied to the interior by the upper DWBC at the crossover.

The mean potential vorticity for the deepest layer is shown in Fig. 3b. It is dominated by β in the domain interior and by the topographic slope along the western boundary.

3) AGE TRACER

The mean value of the age tracer for layer 2 is shown in Fig. 4a. The DWBC is characterized by low age values, increasing from zero at the northern boundary to just over 2 years of age at the northern side of the crossover. It is clear that the upper core of the DWBC is strongly interacting with the basin interior. There is a strong exchange between the DWBC and the interior at the crossover point and a weaker exchange all along the DWBC to the north of the crossover. Near the crossover, the tracer reflects the two mean paths followed by the DWBC. There is a plume of relatively young water leaving the western boundary at the crossover and extending 1500 km into the interior under the Gulf Stream. This indicates that the upper core of the DWBC strongly influences the tracer values under the Gulf Stream. If there were no exchange, the age here would be 17.5 years, as found in the eastern basin. This mean value of less than 8 years represents a quasi-steady balance under the Gulf Stream and is not overly sensitive to further integration of the model. The direct southward path of the DWBC water is also evident in the age tracer as a plume extending to the south from the crossover, as was found in the Q and ψ fields.

The mean age tracer in the deepest layer is shown in Fig. 4b. In contrast to the middle layer, the tracer in the abyssal layer shows very little penetration into the basin interior. The age in the lower DWBC is relatively young all along the western boundary and gradually increases to approximately 4 years at the southern outflow. There is only a weak exchange between the lower DWBC and the interior both at the crossover and adjacent to the northern recirculation gyre. This lack of penetration into the interior indicates that the spreading of the low age tracer into the interior in layer 2 is not a result of the subgrid-scale mixing parameterization in the model, which is the same strength in both layers.

The lack of additional water mass sources and vertical mixing results in a continual increase in the age of the interior waters in both layers; thus, the absolute age in the interior is not as meaningful as the contrast in age between the DWBC and the interior. However, 100-year integrations in Part II demonstrate that the regions influenced by the advective fields along the western boundary current and beneath the Gulf Stream reach a quasi-equilibrium state in 10 to 20 years.

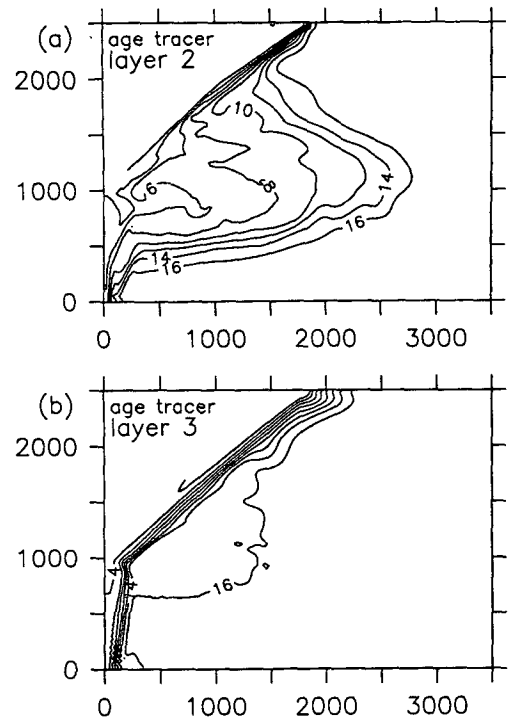

FIG. 4. Time averaged age tracer (years 15 to 20) for the central case with $\tau_m = 0.75$, $\Gamma = (25, 10, 10)$: (a) layer 2 and (b) layer 3.

b. *Entrainment dynamics*

The basic mechanism for the entrainment of upper DWBC water beneath the eastward flowing Gulf Stream is now presented for the central case. Sensitivity experiments in the following section demonstrate the general applicability of these processes to the crossover dynamics.

The upper DWBC water is deflected off the western boundary by approximately 200 km at the crossover between the Gulf Stream and the DWBC (Fig. 2b). While small, it will be shown that this diversion of the upper flow is key to the entrainment and resulting eastward flow of the upper DWBC. The diversion of the upper DWBC arises as a result of the sloping main thermocline associated with the Gulf Stream leaving the shelf. This change in the thickness of the upper layer is seen by the intermediate layer as an increase in potential vorticity along the boundary. The low q waters of the upper DWBC turn offshore upon encountering the potential vorticity gradient. The water is able to continue toward the south only by sliding down the sloping interface between layers 2 and 3, thus maintaining its thickness as the interface between layers 1 and 2 deepens under the Gulf Stream. The interface between layers 2 and 3 must slope downward to the

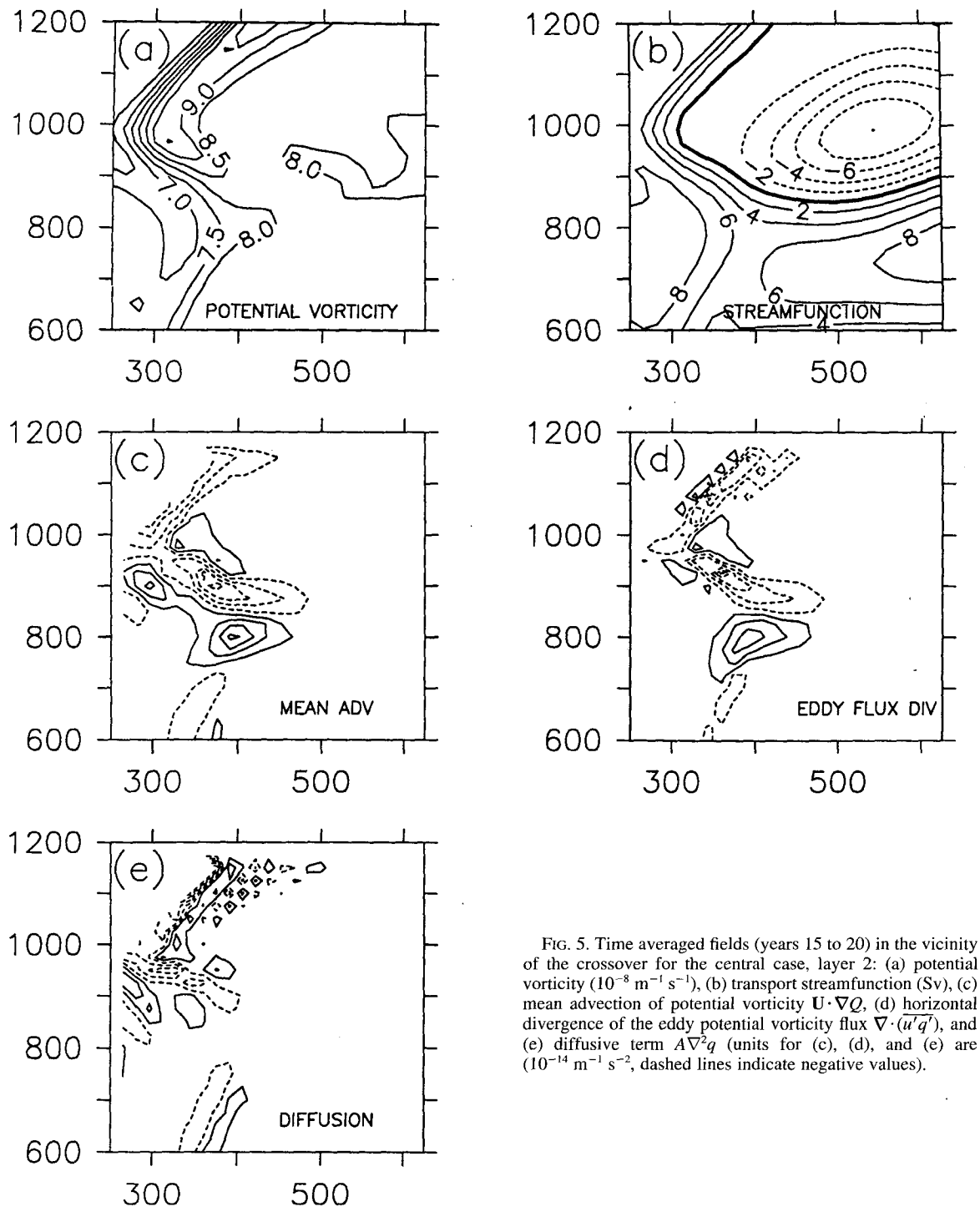

FIG. 5. Time averaged fields (years 15 to 20) in the vicinity of the crossover for the central case, layer 2: (a) potential vorticity (10^{-8} m^{-1} s^{-1}), (b) transport streamfunction (Sv), (c) mean advection of potential vorticity $\mathbf{U}\cdot\nabla Q$, (d) horizontal divergence of the eddy potential vorticity flux $\nabla\cdot(\overline{u'q'})$, and (e) diffusive term $A\nabla^2 q$ (units for (c), (d), and (e) are (10^{-14} m^{-1} s^{-2}, dashed lines indicate negative values).

east in order to balance the transport of the lower DWBC through the thermal wind relation. This is similar to the mechanism proposed by Hogg and Stommel (1985) as a means for the lower DWBC to cross under the Gulf Stream while conserving its potential vorticity. In that case the downward slope was provided by the bottom topography, while here it is provided by the baroclinic flow in the deepest layer. There is no requirement in the three-layer model that the deepest layer slide down the topography at the crossover as it is shielded from the direct influence of the Gulf Stream by the intermediate layer. This pattern agrees well with

the observations of PS93, where the upper DWBC turns sharply offshore at the crossover while the lower DWBC more closely follows the bottom topography.

Figures 5a,b show the mean potential vorticity and transport streamfunction in the vicinity of the crossover. The low Q water indicative of the upper DWBC is seen entering along the western boundary from the north. At the crossover the low Q water comes off the boundary, first toward the southeast, and at 800-km latitude it turns back toward the southwest. The transport streamfunction indicates that the upper DWBC splits into two mean paths at 800-km latitude, with the eastward flow emanating from the easternmost extension of the low potential vorticity tongue. The mean flow of the upper DWBC crosses the mean potential vorticity gradient at this splitting point. The strength and location of this interaction is indicated by $\mathbf{U}\cdot\nabla Q$ and shown in Fig. 5c, where $\mathbf{U}$ is the mean horizontal velocity vector. The value of the potential vorticity at the core of the upper DWBC increases ($\mathbf{U}\cdot\nabla Q > 0$) along the core of the upper DWBC, especially so at the point where the upper DWBC splits into two branches. A similar advection across the potential vorticity field was observed by PS93. The value of Q decreases as the parcels move along the coastline north of the crossover and through the recirculation just to the north of the splitting point. The terms responsible for these changes in the mean potential vorticity are now described.

In a steady, adiabatic, inviscid model this mean flow across potential vorticity contours would not be possible; its existence implies that some nonconservative process is active. Rhines and Holland (1979) showed that the horizontal divergence of the eddy potential vorticity flux can drive a mean flow across lines of constant Q which, in a statistical steady state, may be written as

$$\mathbf{U}\cdot\nabla Q = -\nabla\cdot(\overline{\mathbf{u}'q'}) + A_m\nabla^2(\mathbf{k}\times\nabla V)/h^2, \quad (3)$$

where $\mathbf{u}'$ is the perturbation velocity, and $q' = (f + v_x - u_y)/h - Q$ is the perturbation potential vorticity. A diffusive term proportional to the Laplacian of the horizontal transport has also been retained, consistent with the model numerics. Rhines and Holland (1979) termed the inviscid balance the turbulent Sverdrup balance, where the mean flow across mean potential vorticity contours is maintained by the horizontal divergence of the eddy potential vorticity flux. In the vicinity of the Gulf Stream, Holland and Rhines (1980) found that the eddy potential vorticity flux was dominated by the stretching term (the Reynolds stress term being much smaller) and responsible for the spin up and maintentance of recirculation gyres that are found to the north and south of the Gulf Stream.

The eddy flux term [first term on the right-hand side of Eq. (3)] is shown in Fig. 5d. The large region of positive contours occurs just at the location where the mean transport flows to the east, crossing the mean potential vorticity contours. From Eq. (3), one can see that this will tend to force a mean flow up the mean potential vorticity gradient, or from a region of low Q into a region of high Q. This is the sense that the eastward mean flow takes as it splits and flows to the east. The pattern and magnitude are consistent with the calculated mean flow across the Q contours in Fig. 5c [left-hand side of Eq. (3)]. The eddy flux forcing is small to the south, where the mean flow is approximately along lines of constant Q. The negative region of eddy forcing along the northern recirculation tends to force a mean flow down the Q field, also from the western boundary toward the interior because it is acting on a region of local maximum potential vorticity. The diffusive term arising from the subgrid-scale mixing of horizontal transports [second term on the right-hand side of Eq. (3)] forces the remainder of the mean flow across the mean Q contours, as is shown in Fig. 5e. It is largest near the western boundary; however, in the interior and near the splitting of the upper DWBC, the contribution due to subgrid-scale mixing is negligible.

The change in potential vorticity that would be induced by diapycnal mixing along this diverted path of the upper DWBC may be estimated as

$$\frac{\delta q}{Q} = \frac{KL}{H^2U'}, \quad (4)$$

where δq is the change in potential vorticity in layer 2 due to diapycnal mixing, Q the potential vorticity of layer 2, K the diapycnal mixing coefficient, L the downstream length scale of the recirculation gyres, H the thickness of layer 2, and U is the downstream velocity in layer 2. Assuming typical values of $K = 10^{-4}$ m^2 s^{-1}, $L = 10^6$ m, $H = 10^3$ m, and $U = 10^{-1}$ cm s^{-1} gives $\delta q/Q = 10^{-3}$. This is two orders of magnitude less than the potential vorticity anomaly of the entrained DWBC water, which is about 10% of Q, so the neglect of diapycnal mixing seems reasonable.

The entrainment is not simply a result of the upper DWBC being diverted sufficiently offshore as the eddy flux mechanism is necessary for driving the mean flow across mean potential vorticity contours. This conclusion is verified by a calculation with a sufficiently large horizontal diffusion ($A_m = 1500$ m^2 s^{-1} and all other forcing parameters as in the central case) such that eddy formations are suppressed. In this case the upper DWBC is diverted offshore at the crossover but all of the transport returns to the western boundary without getting entrained under the Gulf Stream.

Additional insight into the mechanism of the eddy flux forcing is revealed by a synoptic picture of the potential vorticity shown in Fig. 6a. Although there is much more variability than for the mean potential vorticity field, the same basic characteristics of the field remain: the low q in the upper DWBC, the high q adjacent to the upper DWBC, and the homogenized region under the Gulf Stream. The eddy flux of potential vorticity is achieved by the shedding of patches of low

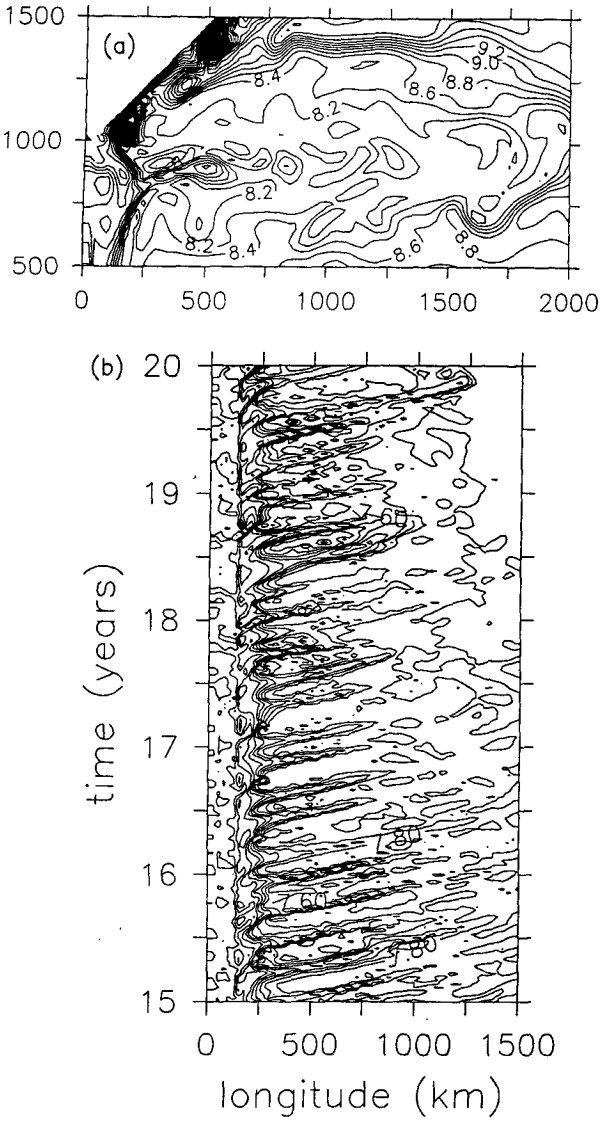

FIG. 6. (a) Synoptic field of potential vorticity of layer 2 near the crossover for the central case. (b) Minimum value of the potential vorticity in layer 2 as a function of time and longitude (10^{-8} m^{-1} s^{-1}).

q water from the upper DWBC at the crossover point. One such anomalous patch is just separating from the upper DWBC at about 500-km longitude, 850-km latitude in Fig. 6a. This anomalous water is essentially pulled from the upper DWBC by the northern and southern recirculation gyres as the upper DWBC is diverted toward the interior at the crossover. The recirculation gyres are not evident in the potential vorticity field because they are nearly barotropic. The anomalous patch of low q is then carried toward the east by the eastward flowing deep Gulf Stream. Anomalous patches are also evident at longitudes of 800 km, 1250 km, and 1700 km from previous separation events. The negative eddy flux divergence in Fig. 5d results from the eastward transport of low q patches of upper DWBC water from the splitting point, which acts to increase the mean potential vorticity of the upper DWBC while reducing the mean Q under the Gulf Stream. Similar trends in potential vorticity tendency along Lagrangian trajectories are found in the data analysis of PS93.

The frequency of such events, and their downstream propagation, are indicated in Fig. 6b. This shows the minimum value of the potential vorticity in layer 2 between latitudes 600 km and 1100 km as a function of time and longitude. The mean upper DWBC is characterized by the low q water within 200 km of the western boundary. The eddy formation events are indicated by patches of low q propagating toward the interior from the western boundary about once every three months. They clearly propagate to the east with a speed of about 9 cm s^{-1}. The influence of mixing with the interior results in an erosion of the minimum value of q as the eddies propagate offshore. They are no longer distinguishable from the background at approximately 1500-km longitude.

This eddy flux mechanism for driving a branching of the DWBC into interior recirculation gyres is quite different from the wave-driven recirculation gyres that result from instabilities of the Antarctic Bottom Water DWBC in the Brazil Basin discussed by Spall (1994). That mechanism is not effective here because the lower DWBC is locally stable at all latitudes due to the steep topographic slope.

A scaling estimate of the mean flow driven by the eddy potential vorticity flux is now made. The flux is dominated by the stretching term so that

$$\overline{u'q'} \approx \frac{\overline{u'h'Q}}{H}, \tag{5}$$

where h' is the perturbation layer thickness. The transport E induced by the eddy fluxes is calculated using Eq. (3) as

$$E = UL_EH = \frac{u'h'L_MH}{\delta h}, \tag{6}$$

where L_E is the horizontal scale over which the eddy fluxes are active, L_M is the horizontal scale over which Q varies, and δh is the difference in the isopycnal layer thickness between the upper core of the DWBC and the basin interior. For the central experiment, $u' = 3$ cm s^{-1}, $h' = 100$ m, $L_M = 200$ km, $H = 1000$ m, and $\delta h = 100$ m. This gives a total transport across the mean Q contours of 6 Sv in general agreement with their observed diversion of upper DWBC water in Fig. 2. In addition, the amplitude of the eddy flux found here ($u'h' = 3$ m^2 s^{-1}) is very similar to the amplitude estimated from a three-year time series at 73°W. PS93 calculated the eddy heat flux to be approximately 10°C cm s^{-1}. This may be converted into the eddy thickness flux used in the above scaling by dividing by the ver-

tical temperature gradient, which is approximately 0.02°C m^{-1}, giving an eddy thickness flux of $u'h' \approx 5\ m^2\ s^{-1}$. This estimate is only approximate, and the data were not acquired exactly at the crossover; however, it does show that the observed eddy activity is of the same order of magnitude as that produced in the model. In fact, PS93 hypothesized that this eddy flux term might be responsible for the observed flow across q contours; however, the data was insufficient to fully test this hypothesis. One important difference between the present model results and their data analysis is that the synoptic model fields very nearly conserve potential vorticity following the synoptic flow. The mean flow across the mean potential vorticity fields is only apparent after the time average is taken, while the data of PS93 was nearly synoptic. Perhaps the spatial smoothing in PS93 has somehow approximated the temporal smoothing taken here.

c. *Sensitivity to forcing*

The sensitivity of the entrainment process to variations in the upper-layer forcing (wind stress amplitude and Gulf Stream inflow transport), intermediate-layer forcing (upper DWBC transport), and lower-layer forcing (lower DWBC transport and bottom topography) is now presented.

1) UPPER-LAYER FORCING

The sensitivity of the intermediate and deep circulations to the upper-layer forcing is now explored. The mean transport streamfunction in layer 2 is shown in Figs. 7a,b for maximum surface wind stresses of $\tau_m = 1.0$ dyn cm^{-2} and $\tau_m = 0.5$ dyn cm^{-2}, respectively. The case with increased surface wind stress drives stronger recirculation gyres (about 12 Sv in each), as expected for an increased transport in the upper ocean Gulf Stream and the resulting increase in the eddy flux mechanism that is responsible for the existence of the recirculation gyres. There is also an increased entrainment of the upper core of the DWBC such that essentially all of the DWBC transport now flows eastward under the Gulf Stream. All of this transport diverted at the crossover returns to the western boundary south of the southern recirculation gyre. About 2 Sv of DWBC water is still diverted into the interior north of the northern recirculation gyre and carried to the eastern boundary before flowing out the southern boundary, as found in the central case. Figure 7b indicates that decreasing the surface wind stress results in weaker recirculation gyres (approximately 5 Sv in layer 2) and an increase in the transport of the DWBC that flows directly to the south without getting entrained under the Gulf Stream. These results are consistent with the eddy fluxes at the crossover being driven by the interaction of the recirculation gyres with the upper DWBC. Although extensive calculations have not been done, the splitting

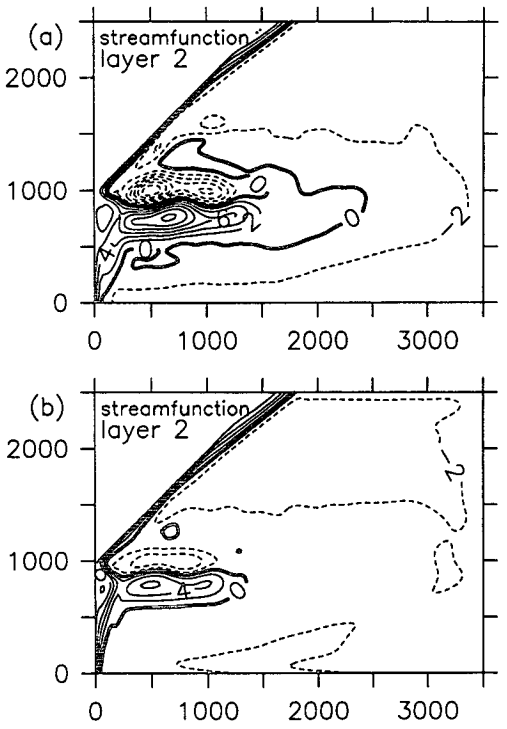

FIG. 7. Sensitivity of layer 2 mean transport streamfunction (years 15 to 20) to surface wind stress: (a) $\tau_m = 1.0$ and (b) $\tau_m = 0.5$ [$\Gamma = (25, 10, 10)$ in both cases].

mechanism does not seem to be overly sensitive to the latitude of the zero in wind stress curl. A northward shift of 500 km in the zero wind stress curl latitude simply shifts the Gulf Stream separation, and location of the DWBC splitting, to the north.

The inflow transport of the Gulf Stream has two influences on the entrainment of upper DWBC water. First, an increased transport results in a more unstable Gulf Stream, larger eddy fluxes, stronger recirculation gyres, and larger entrainment at the crossover. Second, an increased transport must be balanced by a larger cross-stream change in the thickness of layer 1, and thus results in a larger offshore shift in the upper DWBC at the crossover as it tries to conserve its potential vorticity. Each of these changes tends to increase the eddy flux mechanism discussed previously and drive a larger mean flow from the upper DWBC into the interior under the Gulf Stream. Figure 8a shows the layer-2 mean transport streamfunction for an inflow transport $\Gamma_1 = 50$ Sv. As expected, now essentially all of the upper DWBC water is diverted into the interior. Decreasing the transport of the Gulf Stream that flows into the model domain from the west results in a more stable Gulf Stream, weaker eddy-driven recirculation gyres, and a smaller offshore shift in the upper DWBC. For a case with no inflow coming off the shelf $\Gamma_1 = 0$ Sv (Fig. 8b), the (purely wind-driven) Gulf Stream has only very small, weak recirculation gyres and entrains

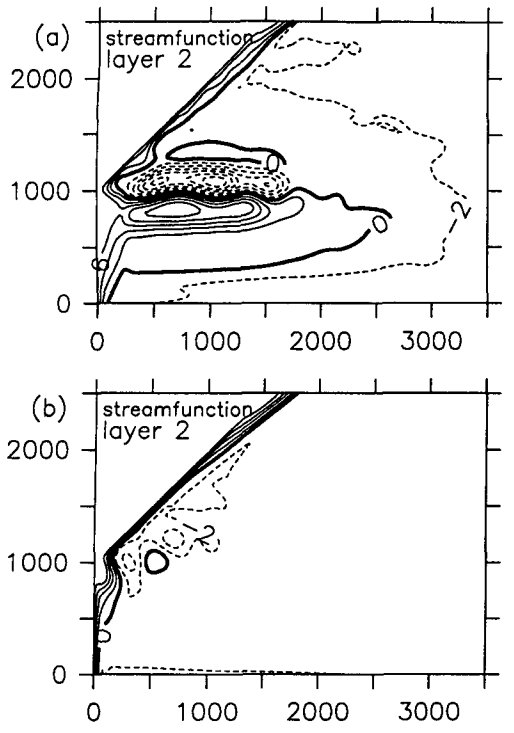

FIG. 8. Sensitivity of layer 2 mean transport streamfunction (years 15 to 20) to Gulf Stream transport off the shelf: (a) Γ = (50, 10, 10) and (b) Γ = (0, 10, 10) (τ_m = 0.75 in both cases).

no DWBC water in this layer. There is still a slight diversion of the upper DWBC water off the boundary due to the sloping thermocline that arises from the wind-driven Gulf Stream transport.

Although the properties of the Gulf Stream inflow are held steady in time, it is possible that feedbacks between the crossover dynamics and the position, angle, or transport of the Gulf Stream may introduce some additional time dependence or low-frequency oscillations in the behavior of the upper DWBC.

2) UPPER DWBC TRANSPORT

The mean transport streamfunction in the surface layer for the central case is shown in Fig. 9a, along with the mean surface layer transport streamfunction for a case with no upper DWBC inflow in Fig. 9b. The mean path of the Gulf Stream in the absence of the upper DWBC transport separates from the coast approximately 250 km to the north (near the latitude of zero wind stress curl) compared to the case with 10 Sv of upper DWBC transport. Influences of the DWBC on the Gulf Stream separation were also found in the models of TS89 and Ezer and Mellor (1992). The study of TS89 had only two layers, with the DWBC confined to the deepest layer, while Ezer and Mellor specified a barotropic inflow at high latitudes and an outflow through the eastern boundary to represent the northern recirculation gyre. The present calculations still carry 10 Sv of lower DWBC water. The large response in Gulf Stream separation and interior path is found for a relatively small decrease in the upper DWBC transport of only 10 Sv [although a large percentage (50%) of the total DWBC transport], while TS89 and Ezer and Mellor (1992) found similar shifts in the mean Gulf Stream path for changes of 40 Sv (100% of the total DWBC transport).

The reason for this increased sensitivity is easily understood if we consider the interaction of the DWBC and the Gulf Stream at the crossover by invoking the process discussed by TS89. The southward shift of the

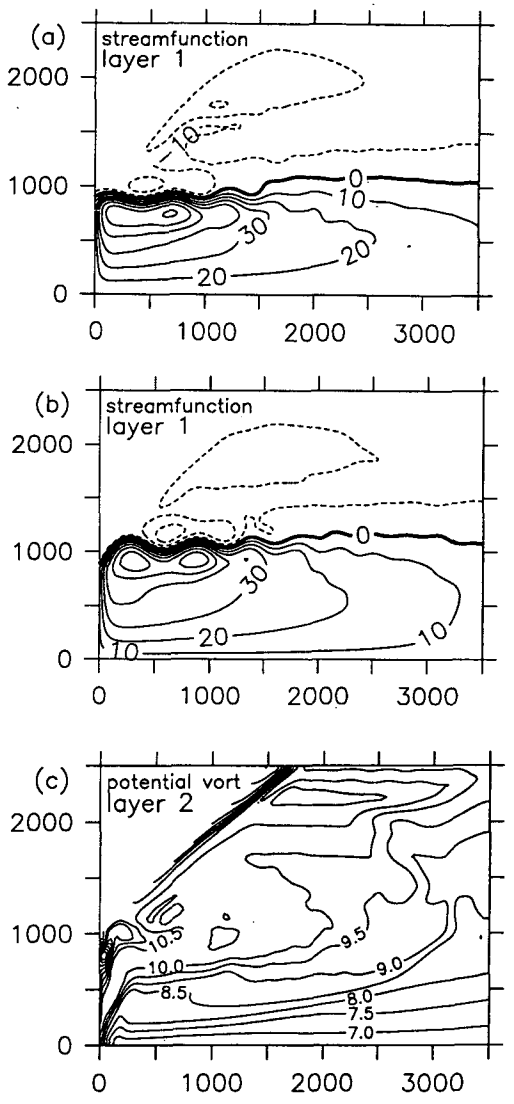

FIG. 9. Sensitivity of layer 1 mean transport streamfunction (years 15 to 20) to upper DWBC transport: (a) the central case [Γ = (25, 10, 10)], (b) with no inflow transport in the upper DWBC (Γ = (25, 0, 10)), and (c) mean potential vorticity in layer 2 for no inflow transport in the upper DWBC.

separation point is a result of the southward flowing DWBC essentially advecting the sloping interface of the Gulf Stream to the south through the term $\mathbf{v}\cdot\nabla h$ in the continuity equation. Because TS89 had only one layer to represent the DWBC, their change of 40 Sv of DWBC transport resulted in a change of the velocity in the DWBC of approximately 6 cm s^{-1} (assuming a depth of 3000 m and a boundary current width of 200 km. The 10-Sv change in the transport of the intermediate layer results in a similar change in the velocity of the upper DWBC of 5 cm s^{-1} because the transport is distributed over only 1000-m depth. Thus, the increased vertical resolution results in an increased sensitivity in the Gulf Stream separation to the transport of the DWBC; however, the momentum imparted on the Gulf Stream by the DWBC is approximately the same in both cases. This allows for large shifts in the Gulf Stream separation latitude for changes that are within reasonable uncertainties for the mean or for temporal fluctuations in the DWBC transport. This result also identifies the upper core of the DWBC as being more important than the deep core in influencing Gulf Stream separation, although the deep core is indirectly important through its influence on the upper DWBC pathway (see next section).

The potential vorticity in layer 2 is strongly influenced by the upper core of the DWBC as a result of the crossover. The potential vorticity in layer 2 for the case with no upper DWBC inflow is shown in Fig. 9c (compare with Fig. 3a for the central case). There is still a large region of homogenized Q, but its value is now approximately 20% larger than for the central case. This is primarily reflected by a smaller layer thickness under the Gulf Stream for layer 2, a decrease from 1175 m to 875 m. This indicates that the entrainment of upper DWBC water under the Gulf Stream has modified the basin-scale stratification below the main thermocline. The influences of this low potential vorticity on the stability and time-dependent behavior of the Gulf Stream is the subject of a companion paper (Spall 1996). The spatial influence of the low Q in the upper DWBC is similar to that found for the age tracer and is as expected for other tracers such as temperature and salinity.

3) Lower DWBC transport

Although the lower DWBC is not strongly affected by the Gulf Stream at the crossover, it does have an important influence on the transport of the upper DWBC and the Gulf Stream. The mechanism of upper DWBC entrainment involves the divergence of eddy potential vorticity fluxes at the crossover driving a mean flow across the mean potential vorticity contours. The eddy fluxes arise from the interior recirculation gyres pulling off patches of upper DWBC water after the upper DWBC has been diverted toward the interior. This offshore turning is important for the eddy flux mechanism because it allows the interior recirculation gyres to interact more strongly with the upper DWBC. The further offshore the upper DWBC extends, the stronger the interaction with the interior recirculation gyres and the larger the eddy flux.

The distance the upper DWBC flows offshore is partially controlled by the steepness of the interface slope between layers 2 and 3 (and also the potential vorticity gradient imposed by the upper ocean Gulf Stream, as discussed previously). If the interface is weakly sloping, the upper DWBC must flow farther offshore before crossing under the Gulf Stream in order to conserve its layer thickness. On the other hand, a strongly sloping interface will allow the upper DWBC to turn southward after shifting offshore by only a small amount. The steepness of the slope between layers 2 and 3 is controlled by the thermal wind relation, or in other words, the vertical shear in velocity between layers 2 and 3. Thus, one expects that for a stronger transport in layer 3 the upper DWBC will be diverted less at the crossover and the interaction with the interior recirculation gyres will be lessened and the resulting decrease in eddy fluxes will force a weaker mean flow into the interior. This is just what is found for a case with 20 Sv in the lower DWBC, as indicated by the transport streamfunction for layer 2 shown in Fig. 10. For a calculation with zero lower DWBC transport all of the upper DWBC is entrained offshore, similar to the flat bottom case in the next section.

4) Bottom topography

The continental slope plays an important role in the dynamics of the lower DWBC and, indirectly, the upper DWBC and Gulf Stream. The sloping topography provides a means for the lower DWBC to flow toward the equator while nearly conserving its potential vorticity by allowing the current to ride up the slope, thus diminishing its layer thickness to balance the decrease in the Coriolis parameter, yet accelerating the flow in order to maintain its transport (Spall 1994). In the absence of this slope, the lower DWBC can remain flow-

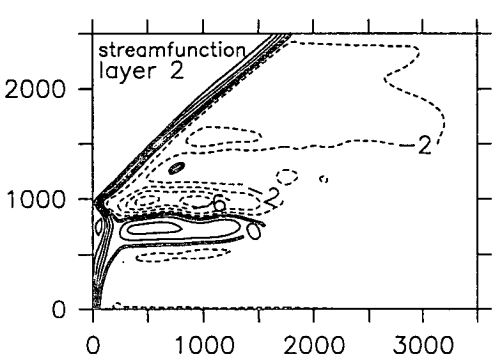

FIG. 10. Mean transport streamfunction (years 15 to 20) in layer 2 for a lower DWBC inflow transport of 20 Sv, all other parameters as in the central case.

ing southward through the crossover point as a western boundary current and still conserve potential vorticity, through the generation of relative vorticity. A calculation with a flat bottom and Γ = (25, 10, 10) Sv was carried out. The mean streamfunction in layers 2 and 3 are shown in Figs. 11a,b. The lower DWBC no longer remains on the western boundary but flows into the interior both north of the crossover and at the crossover. The entire lower DWBC turns offshore between two recirculation gyres. The lack of the continental slope allows the recirculation gyres to develop adjacent to the coastline and thus maximizes their interaction with the western boundary currents. After recirculating around the southern gyre, the lower DWBC flows to the south in a very narrow boundary current. The increase in potential vorticity resulting from the southward flow south of the crossover is balanced by the generation of relative vorticity and lateral diffusion.

The influences of the bottom topography are not confined to the lowest layer. The western intensification of the lower DWBC in the presence of the sloping bottom allowed the upper DWBC to cross under the Gulf Stream while approximately conserving its potential vorticity (in the absence of the eddy fluxes). Once the lower DWBC is turned offshore at the crossover, the sloping interface between layers 2 and 3 is no longer present and the upper DWBC cannot flow to the south at the crossover point withough generating unrealistically large anticyclonic relative vorticity $[0(-0.5f)]$ to compensate for the decrease in layer thickness. As a result, the entire upper DWBC is also turned offshore at the crossover. This complete entrainment of the upper DWBC is also found for a case with a sloping bottom but with zero transport in the lower DWBC for the same reason, the loss of the sloping interface between layers 2 and 3 that provided a means for the upper DWBC to cross under the Gulf Stream.

d. DWBC entrainment and DWBC age

The sensitivity of the upper DWBC transport to variations in the model forcing may be summarized by two indices: 1) the amount of upper DWBC water entrained under the Gulf Stream and 2) the age of the upper DWBC water south of the crossover. Figure 12a shows the amount of upper DWBC that gets entrained into the interior (maximum value of 10 Sv) versus the strength of the eddy-driven recirculation gyres in the interior of the basin. The square marks the central case, while circles of increasing size indicate increasing maximum wind stress, triangles correspond to the amplitude of the Gulf Stream inflow transport, and crosses correspond to the amplitude of the lower DWBC. There is an approximately linear increase in the amount of upper DWBC entrained with increasing strength of the recirculation gyres as a result of changes in the surface wind stress (all other parameters are as in the central case). The calculation with an increased inflow Gulf Stream

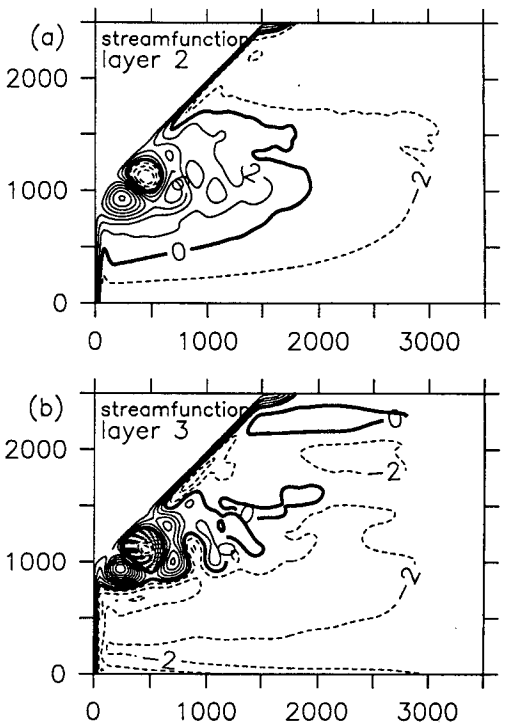

FIG. 11. Mean transport streamfunction (years 15 to 20) for case with a flat bottom: (a) layer 2 and (b) layer 3. All other parameters as in the central case.

transport (large triangle) results in a larger entrainment for the same strength of the recirculation gyres when compared to the central case. This result is because the larger Gulf Stream transport forced the upper DWBC to flow farther into the interior in an attempt to conserve its potential vorticity and, as a result, it produces larger eddy fluxes at the crossover. Similarily, the case with decreased Gulf Stream transport (small triangle) results in less entrainment than would be expected for similar strength recirculation gyres with the central Gulf Stream inflow. Increasing the transport in the deepest layer inhibits the entrainment of upper DWBC (large cross) because the upper DWBC does not flow as far offshore at the crossover and the interaction with the interior recirculation gyres is lessened. Decreasing the transport in the deepest layer (small cross) enhances the entrainment of upper DWBC water for similar strength recirculation gyres because the upper DWBC flows farther offshore as it slides down the interface slope between layers 2 and 3.

A representative age of the upper DWBC south of the crossover has been calculated as

$$\bar{A} = \frac{\int_0^x Auhdx}{\int_0^x uhdx}, \tag{7}$$

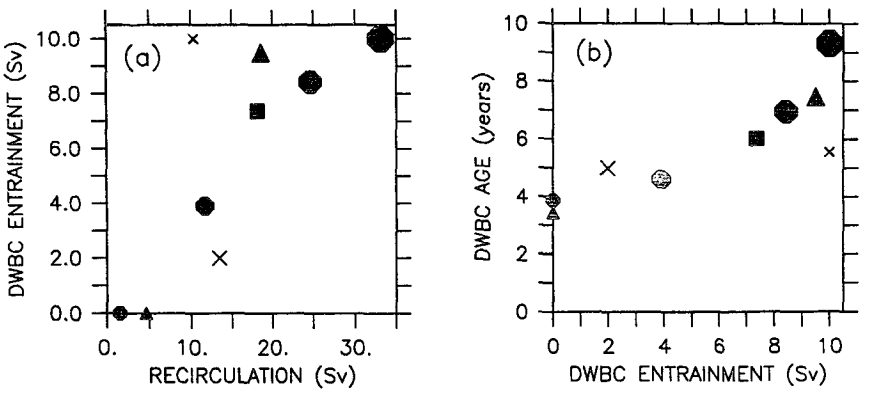

FIG. 12. (a) Amount of upper DWBC water entrained under the Gulf Stream versus the strength of the interior recirculation gyres. (b) Age of the upper DWBC south of the crossover versus the amount of upper DWBC water entrained under the Gulf Stream. The symbols correspond to: square—the central run with $\Gamma = (25, 10, 10)$, $\tau_m = 0.75$; circles—increasing size for $\tau_m = 0.25$, 0.5, 1.0, 1.5; triangles—$\Gamma_1 = 0$ Sv (small) and $\Gamma_1 = 50$ Sv (large); crosses—$\Gamma_3 = 0$ Sv (small) and $\Gamma_3 = 20$ Sv (large).

where A is the value of the mean age tracer. The integral was taken along the southern boundary of the domain between $x = 0$ and 500-km longitude. The outflow age in the upper DWBC for a calculation with no upper-layer forcing is 2.5 years. Taking a distance traveled from the northern inflow of 3200 km, this gives an effective speed of 4.1 cm s^{-1}. The actual maximum speed in the upper DWBC along the western boundary averaged 11.5 cm s^{-1}. The difference between these two velocities can be attributed in part to the subgrid-scale mixing of the age tracer with the older values in the interior along the path of the DWBC. Of course, even in the absence of mixing, one would expect the effective speed to be less than the maximum speed because the effective velocity is representative of the average DWBC speed. An average speed, taking the DWBC width as 200 km, would be approximately 5 cm s^{-1}.

The influence of the entrainment forced by the Gulf Stream is indicated by the increase in outflow ages to between 3.5 and 9.3 years for the various experiments, as shown in Fig. 12b. There is an increase in the effective age of the upper DWBC water as more amounts of the upper DWBC water get entrained under the Gulf Stream. This results both from an increased pathlength due to the diversion, and from mixing with older, unventilated waters in the basin interior. For the case of maximum Gulf Stream entrainment, the effective velocity is decreased to approximately 0.9 cm s^{-1}. The entrainment of upper DWBC water at the crossover has a large influence on the effective age of the water south of the crossover. For parameters representative of the real North Atlantic Ocean, the entrainment causes a decrease in the effective velocity of the upper DWBC by a factor of 2–3.

4. Relation to observations

The results found in the model calculations are consistent with a variety of observational results. The circulation patterns in both the upper DWBC and lower DWBC at the crossover are remarkably similar to the synoptic estimates of PS93. The main features that they find in the intermediate layer are that all of the DWBC flows off the boundary at the crossover (crossing potential vorticity contours), some of this continues to the south while the remainder flows to the east under the upper ocean Gulf Stream. This circulation pattern is also suggested by the lateral distribution of CFCs, which shows two tongues of relatively high concentration: one extending under the upper ocean Gulf Stream at the crossover and the other extending to the south along the boundary. Their circulation pattern also suggests a large exchange with the interior, with inflow from offshore turning both north under the Gulf Stream and south with the DWBC. This is essentially the same pattern found in the time-mean streamfunction for most of the model calculations. The deep DWBC circulation and CFC data of PS93 indicates that most of the current flows straight to the south along the topography and does not turn offshore under the Gulf Stream. There is also weaker exchange with the interior both north and south of the crossover. This circulation pattern is also quite similar to the mean flow produced by the model. It should be noted that the model results presented here are 5-year averages, while the data of PS93 are synoptic (though spatially smoothed). However, the mean splitting patterns found near the crossover in the model are also visible in the synoptic fields, while the interior circulations in the intermediate and deep layers are often dominated by the eddy variability.

PS93 also find an abrupt change in the properties of the upper DWBC at the crossover. The sense of the change is that the upper DWBC becomes warmer, saltier, and lower in CFCs. Both the pattern of circulation and the change in properties of the upper DWBC are consistent with the splitting of upper DWBC water at the crossover, its mixing with interior water under the Gulf Stream, and its returning to the western boundary south of the crossover as found in the model. The lower DWBC does not exhibit such an abrupt change in properties at the crossover, although it is not clear if this is due to lack of exchange or that the properties of the interior are similar to the DWBC properties in this density layer. The analysis of Doney and Jenkins (1994) indicates a remarkably uniform increase in the age of the lower DWBC water with distance from its source, also suggesting little interaction at the crossover. These findings are consistent with the model result that the lower DWBC has little exchange with the interior at the crossover.

There is some evidence of a high CFC core in the density range of the upper DWBC to the east of the crossover in the sections of Smethie (1993). A section at 55°W shows a local maximum in F-11 at a depth of 1000 m–1500 m just south of the Gulf Stream. The spatial coverage of the data is not really sufficient to determine where this high F-11 water originated. One possibility is that it was transported across the Gulf Stream by some diffusive (on the large scale) process such as through cold ring formation events. The present results, together with the results of PS93, suggest that this water crossed the stream at the western boundary crossover and was carried to the east in the southern recirculation gyre. Doney and Jenkins (1994) tritium–helium age estimates show recently ventilated waters under the Gulf Stream and in the recirculation gyres, but not south of the southern recirculation gyre.

The recent schematic circulation patterns composed by Schmitz and McCartney (1993) indicate a slightly different path for the upper DWBC water. They show a splitting near the Grand Banks with approximately 12 Sv remaining along the western boundary down to the crossover and 4 Sv flowing south from the Grand Banks and rejoining the DWBC south of the crossover. The modification to this pattern implied by the present results would suggest that the flow joining the DWBC south of the crossover had originated from the western boundary at the crossover. There may also be some splitting at the Grand Banks, perhaps controlled by a mechanism similar to the entrainment found here.

5. Conclusions

A regional primitive equation model has been applied to a series of experiments to investigate the dynamics of the Gulf Stream/deep western boundary current crossover. The results indicate that what happens at the crossover can have a significant impact on the properties and pathways of both the Gulf Stream and the DWBC. The upper DWBC can split into two mean paths, one that flows to the east under the Gulf Stream and another that flows to the south along the western boundary. The portion that flows to the east mixes with waters from the gyre interior and is returned to the western boundary current south of the crossover by the southern recirculation gyre. The lower DWBC is only weakly influenced by the crossover, with most of the DWBC water flowing directly to the south. There is an interaction in both DWBC layers with the interior through eddy-driven recirculation gyres. These flow characteristics agree well with recent observations. The entrainment of upper DWBC is driven by eddy fluxes of potential vorticity at the crossover point. This eddy flux is characterized by patches of low potential vorticity water separating from the upper DWBC and being advected into the interior under the Gulf Stream by the recirculation gyres. A consistent picture emerges from sensitivity experiments in which more upper DWBC water is entrained for an increase in the strength of the Gulf Stream or for a decrease in the strength of the lower DWBC. The surface wind stress and transport of the Gulf Stream separating from the continental shelf can thus indirectly ventilate the intermediate layers of the North Atlantic Ocean through entrainment and mixing of the upper DWBC water.

The presence of the upper DWBC has a large influence on the path of the Gulf Stream, qualitatively consistent with previous modeling studies. One notable difference is that the large shift in the separation latitude of the Gulf Stream (250 km) is found here for a change in the upper DWBC transport of only 10 Sv, compared with 40 Sv changes in previous studies. This increased sensitivity is attributed to the increased vertical resolution of the DWBC. The entrainment also has large consequences on the basin-scale stratification below the main thermocline as the entrained DWBC water significantly reduces the potential vorticity of the intermediate layers, compared to cases where there is no upper DWBC or the eddy fluxes are not sufficient to entrain the upper DWBC under the Gulf Stream. The properties of the upper DWBC change abruptly for those cases in which the water is entrained at the crossover due to mixing with interior waters under the Gulf Stream. The lower DWBC is not strongly influenced at the crossover due to the presence of the continental slope.

These results suggest that the correct representation of the vertical structure of the DWBC and resolution of the time-dependent, baroclinic entrainment mechanisms at the crossover point may be important factors in developing models of the large-scale circulation and climate. The DWBC, especially the upper layers, do not simply provide a direct connection between their high-latitude source regions and lower latitudes. Mixing with the interior is clearly important in determining the flow pathways and properties and is controlled by

small-scale processes along the western boundary. It is anticipated that similar entrainment mechanisms may exist in other regions where the upper-ocean flow interacts with the intermediate and deep flows, such as near the Grand Banks and where the DWBC crosses the equator. The present results are based on steady forcing; however, it is expected that time-dependent forcing may result in an even more complex interaction between the boundary currents and the interior. The influences of the entrained upper DWBC water on the stability of the Gulf Stream and its ability to force decadal oscillations in the Gulf Stream/DWBC system are the subject of Part II of this study (Spall 1996).

Acknowledgments. This work was supported by the National Science Foundation Grant OCE-9301323 and NOAA Grant NA36GP0309 through the Atlantic Climate Change Program. Calculations were carried out on the Cray YMP at the National Center for Atmospheric Research. Don Olson at the University of Miami also provided some computing resources. Bob Pickart is thanked for numerous interesting and helpful discussions. Harley Hurlburt and Tammy Townsend are thanked for providing the original model code and for answering many questions about the model.

APPENDIX

Model Equations and Boundary Conditions

The model used in this study is described in detail in Thompson and Schmitz (1989) and the references therein. Only a summary of the equations solved by the model and the boundary conditions are included here.

The layer averaged momentum equations for layer k are written as

$$\frac{\partial \mathbf{V}_k}{\partial t} + (\nabla\cdot\mathbf{V}_k + \mathbf{V}_k\cdot\nabla)\mathbf{v}_k + k\times f\,\mathbf{V}_k = -\mathrm{h}_k\nabla P_k + \rho^{-1}(\tau_k - \tau_{k+1}) + A_m\nabla^2\mathbf{V}_k. \quad \text{(A1)}$$

The layer transport is given by $\mathbf{V}_k = h_k\mathbf{v}_k = h_k(u_k\mathbf{i} + v_k\mathbf{j})$. Subgrid-scale processes are parameterized by a Laplacian operation on the horizontal transport with mixing coefficient A_m. The interfacial stresses τ_k are nonzero only at the surface (applied wind stress) and at the bottom (bottom drag). The continuity equation is represented as a prognostic equation for the layer thickness h_k,

$$\frac{\partial h_k}{\partial t} + \nabla\cdot\mathbf{V}_k = 0, \quad \text{(A2)}$$

and the pressure at the interface between layers k and $k+1$ (P_k) is calculated through the hydrostatic equation as

$$P_k = g\eta_1 - \sum_{l=1}^{k-1} g'_k h_k, \quad \text{(A3)}$$

where η_1 is the free surface elevation, g is the gravitational acceleration, and $g'_k = g(\rho_k - \rho_{k+1})/\rho_0$ is the reduced gravity for each layer. There is a quadratic bottom drag applied as

$$\tau_{kk+1} = C_b|\mathbf{v}_{kk}|\mathbf{v}_{kk}, \quad \text{(A4)}$$

where kk is the maximum number of layers and C_b is a bottom drag coefficient.

The transport that is specified to flow into each layer through defined inflow ports must flow out of each layer through open boundary conditions calculated along portions of the model boundaries declared as open. The transport component at each outflow point is first approximated by a radiation condition similar to that proposed by Orlanski (1976),

$$V_B^{n+1} = \left[\left(1 - \frac{c}{c^*}\right)V_B^{n-1} + \left(\frac{2c}{c^*}\right)V_{B-1}^{n}\right]\Big/\left(1 + \frac{c}{c^*}\right), \quad \text{(A5)}$$

where $c^* = \Delta x/\Delta t$ is the horizontal grid spacing divided by the time step, the subscript B indicates the boundary value, $B-1$ is located at one grid point inside the boundary value, and superscripts $n-1$, n, and $n+1$ refer to the previous, present, and next time levels. The phase speed c is defined as

$$c = \min(c^*, \bar{u}_{0k}), \quad \text{(A6)}$$

where $\bar{u}_{0k}$ is the velocity normal to the boundary. A linear drag is then applied to any outflow points that predict an inflow. TS89 found this drag term to be necessary to limit unreasonably large recirculation gyres near the Gulf Stream, although the present results have been found to be insensitive to this drag. The final step is to uniformly accelerate or decelerate the outflow velocity such that the total outflow transport balances the total inflow in each layer (the present model is adiabatic so mass within each layer is conserved). These are the same boundary conditions used by TS89, for more details the reader is referred to their paper and the references therein.

REFERENCES

Agra, C., and D. Nof, 1993: Collision and separation of boundary currents. *Deep-Sea Res.*, **40,** 2259–2282.

Cessi, P., 1991: Laminar separation of colliding western boundary currents. *J. Mar. Res.*, **49,** 697–717.

Chassignet, E. P., and P. R. Gent, 1991: The influence of boundary conditions on midlatitude jet separation in ocean numerical models. *J. Phys. Oceanogr.*, **21,** 1290–1299.

——, and R. Bleck, 1993: The influence of layer outcropping on the separation of boundary currents. Part I: The wind-driven experiments. *J. Phys. Oceanogr.*, **23,** 1485–1507.

Doney, S. C., and W. J. Jenkins, 1994: Ventilation of the deep western boundary current and abyssal western North Atlantic: Estimates from Tritium and ^{3}He distributions. *J. Phys. Oceanogr.*, **24,** 638–659.

Ezer, T., and G. L. Mellor, 1992: A numerical study of the variability and the separation of the Gulf Stream induced by surface atmospheric forcing and lateral boundary flows. *J. Phys. Oceanogr.*, **22,** 660–682.

Fine, R. A., 1995: Tracers, timescales, and the thermohaline circulation: The lower limb in the North Atlantic Ocean. *Rev. Geophys.*, **33**(Suppl.), 1353–1365.

——, and R. L. Molinari, 1988: A continuous deep western boundary current between Abaco (26.5°N) and Barbados (13°N). *Deep-Sea Res.*, **35,** 1441–1450.

Hogg, N. G., and H. Stommel, 1985: On the recirculation between the deep circulation and the Gulf Stream. *Deep-Sea Res.*, **32,** 1181–1193.

Holland, W. R., 1978: The role of mesoscale eddies in the general circulation. *J. Phys. Oceanogr.*, **8,** 363–392.

——, and P. B. Rhines, 1980: An example of eddy-induced ocean circulation. *J. Phys. Oceanogr.*, **10,** 1010–1031.

——, T. Keffer, and P. B. Rhines, 1984: Dynamics of the oceanic general circulation: The potential vorticity field. *Nature,* **308,** 698–705.

Johns, W. E., 1988: One-dimensional baroclinically unstable waves on the Gulf Stream potential vorticity gradient near Cape Hatteras. *Dyn. Atmos. Oceans,* **11,** 323–350.

McDowell, S., P. Rhines, and T. Keffer, 1982: North Atlantic potential vorticity and its relation to the general circulation. *J. Phys. Oceanogr.*, **12,** 1417–1436.

Orlanski, I., 1976: A simple boundary condition for unbounded hyperbolic flows. *J. Comput. Phys.*, **21,** 251–269.

Pickart, R. S., 1992: Water mass components of the North Atlantic deep western boundary current. *Deep-Sea Res.*, **39,** 1553–1572.

——, and W. M. Smethie, 1993: How does the deep western boundary current cross the Gulf Stream? *J. Phys. Oceanogr.*, **23,** 2602–2616.

——, N. G. Hogg, and W. M. Smethie, 1989: Determining the strength of the deep western boundary current using the chlorofluoromethane ratio. *J. Phys. Oceanogr.*, **19,** 940–951.

Rhines, P. B., and W. R. Holland, 1979: Theoretical discussion of eddy-driven mean flows. *Dyn. Atmos. Oceans,* **3,** 289–325.

——, and W. R. Young, 1982: Homogenization of potential vorticity in planetary gyres. *J. Fluid Mech.*, **122,** 347–367.

Schmitz, W. J., and M. S. McCartney, 1993: On the North Atlantic circulation. *Rev. Geophys.*, **31,** 29–49.

Smethie, W. M., 1993: Tracing the thermohaline circulation in the western North Atlantic using chlorofluorocarbons. *Progress in Oceanography,* Vol. 31, Pergamon, 51–99.

Spall, M. A., 1994: Wave-induced abyssal recirculations. *J. Mar. Res.*, **52,** 1051–1080.

——, 1996: Dynamics of the Gulf Stream/deep western boundary current crossover. Part II: Low-frequency internal oscillations. *J. Phys. Oceanogr.*, **26,** 2169–2182.

Thiele, G., and J. Sarmiento, 1990: Tracer dating and ocean ventilation. *J. Geophys. Res.*, **95,** 9377–9392.

Thompson, J. D., and W. J. Schmitz, 1989: A limited area model of the Gulf Stream: Design, initial experiments, and model-data intercomparison. *J. Phys. Oceanogr.*, **19,** 791–814.

Watts, D. R., 1991: Equatorward currents in temperatures 1.8°–6.0°C on the continental slope in the mid-Atlantic Bight. *Deep Convection and Deep Water Formation in the Oceans,* P. C. Chu and J. C. Gascard, Eds., Elsevier, 183–196.